



Novel Sprayable Thermosensitive Benzydamine Hydrogels for Topical Application: Development, Characterization, and *In Vitro* Biological Activities

Muhammet Davut Arpa¹ · Ebrar Elif Kesmen¹ · Sevde Nur Biltekin^{2,3}

Received: 7 July 2023 / Accepted: 3 October 2023

© The Author(s), under exclusive licence to American Association of Pharmaceutical Scientists 2023

Abstract

Benzydamine hydrochloride (BZD) having analgesic, anesthetic, and anti-inflammatory effects is used orally or topically in the treatment of disorders such as joint inflammation and muscle pain. Within the scope of this study, sprayable thermosensitive BZD hydrogels were developed using thermoresponsive poloxamers to avoid systemic side effects and to provide better compliance for topical administration. Also, hydroxypropyl methyl cellulose (HPMC) was employed to improve the mechanical strength and bioadhesive properties of the hydrogel. The addition of BZD generally decreased the viscosity of the formulations ($p < 0.05$), while increasing the gelation temperature ($p < 0.05$). The formulations that did not have any clogs or leaks in the nozzle of the bottle during the spraying process were considered lead formulations. To spray the formulations easily, it was found that the viscosity at RT should be less than 200 mPa·s, and their gelation temperature should be between 26 and 34°C. Increasing HPMC and poloxamer improved bioadhesion. The amount of HPMC and poloxamers did not cause a significant change in the release characteristics of the formulations ($p > 0.05$); the release profiles of BZD from the formulations were similar according to model-independent kinetic ($f_2 > 50$). HPMC and poloxamers had important roles in the accumulation of BZD in the skin. *In vitro* biological activity studies demonstrated that the formulations presented their anti-inflammatory activity with TNF- α inhibition but did not have any effect on the inhibition of COX enzymes as expected. As a result, thermosensitive hydrogels containing BZD might be an appropriate alternative, providing an advantage in terms of easier application compared to conventional gels.

Keywords benzydamine · *in situ* gel · HPMC · poloxamer · thermosensitive hydrogel

Introduction

Benzydamine hydrochloride (BZD) is a non-steroidal drug with anti-inflammatory activity mainly due to its ability to inhibit the production and release of tumor necrosis factor- α (TNF- α) and interleukin-1 β (IL-1 β). BZD, which is administrated both locally and systemically, has analgesic

and anesthetic effects as well. Although BZD is not considered an antibiotic, it is known to have some antimicrobial effects [1, 2]. BZD has different physicochemical and pharmacological properties compared to aspirin-like non-steroidal anti-inflammatory drugs (NSAIDs). Conversely, aspirin-like NSAIDs and their metabolites have an acidic character, whereas BZD is a weak base. The main difference between BZD and other NSAIDs is that BZD has a low inhibitory effect to prevent the production of prostaglandin; however, there are many properties that contribute to its anti-inflammatory activity [3]. BZD is used as mouth spray or mouthwash to treat oromucosal and throat infections and ulcers, besides it is used as a cream, gel, and douche for the treatment of some topical and vaginal conditions [4, 5]. Although BZD is well absorbed in oral administration, the topical applications of its mouthwash, dermal cream, and vaginal douche preparations are known to have weak absorption [6]. Therefore, topical application of BZD can be

✉ Muhammet Davut Arpa
mdarpa@medipol.edu.tr

¹ Department of Pharmaceutical Technology, School of Pharmacy, Istanbul Medipol University, 34815 Istanbul, Turkey

² Department of Microbiology, School of Pharmacy, Istanbul Medipol University, 34815 Istanbul, Turkey

³ Department of Molecular Biology and Genetics, Institute of Graduated Studies in Science, Istanbul University, 34116 Istanbul, Turkey

considered an opportunity since it reduces systemic absorption and minimizes its side effects compared to oral administration [7]. Topical administration of BZD (3% ointment) is effective in conditions such as foot edema [8]. Also, the semi-solid preparations of BZD are used topically for temporary relief of painful and inflamed muscles and joints and breakthrough pain in arthritis and sports injuries [3].

In situ gels, which turn into gel from sol in physiological conditions such as temperature and pH, are drug delivery systems that have been very attractive for the topical application of active ingredients over recent years. Temperature-sensitive *in situ* gels, which are also called thermosensitive hydrogels, undergo gelation with the effect of body temperature [9, 10]. These dosage systems, which offer unique opportunities including longer residence time, higher permeability, easy application, reduced side effects, and minimized systemic absorption, have been recently preferred for topical application to the skin [11–15].

Thermosensitive hydrogels are usually prepared by a technique named cold method using different polymers [16]. The main polymers used in their preparation are Pluronics, also called poloxamers, with synthetic structure and thermoresponsive behavior [17]. Poloxamers are amphiphilic triblock copolymers in the structure of poly(ethylene oxide)–poly(propylene oxide)–poly(ethylene oxide) (PEO–PPO–PEO). Poloxamer 407 (P407) formed of 70%–PEO and 30%–PPO has a high solubility capacity, and poloxamer 188 (P188) formed of 80%–PEO and 20%–PPO is used as an emulsifying, dispersant, and wetting agent and increases the bioavailability of active ingredients with low solubility [18]. These polymers, which have non-ionic and water-soluble properties, interact with hydrophobic surfaces and biological membranes thanks to their amphiphilic characters [19]. Despite their widespread use, poloxamer-based formulations are usually prepared by adding a bioadhesive polymer such as chitosan, HPMC, and Carbopol, due to their weak mechanical strength that causes rapid erosion and low bioadhesive properties of poloxamers [17, 20, 21]. Thus, thanks to polymer blends, it has been possible to combine the advantages of different polymers without the necessity of any chemical modifications [22]. To this end, it was used HPMC, a semi-synthetic polymer, is known as a good bioadhesive and has also thermosensitive sol-gel transition properties [23]. HPMC is a non-toxic, non-ionic, water-soluble polymer and has a good swelling behavior [24]. Hydrogels containing poloxamer and HPMC in combination were presented in the literature. HPMC not only improves the mechanical strength and bioadhesive character of hydrogel but also affects the rheological properties and gelation temperature of hydrogel [22, 23, 25, 26]. The concentration of the polymer, ingredient of solvent, excipients, and temperature of the medium affect the thermo-reversible behavior of HPMC [27].

This work aimed to develop and characterize novel sprayable thermosensitive BZD hydrogels to relieve pain and inflammation in muscles and joints. Furthermore, it was designed to investigate the effects of HPMC used as a bioadhesive agent and the active ingredient used at a high concentration (5%) on the physicochemical properties of the formulation.

Materials and Methods

Materials

BZD was donated from Humanis, Türkiye. P407, P188, and HPMC K4M (medium molecular weight, a viscosity of 4000 mPa·s at 2% in water) were gifted from BASF Chemicals, Germany. Acetonitrile, o-phosphoric acid, sodium dihydrogen phosphate, disodium hydrogen phosphate, benzalkonium chloride, MTT salt, and phosphate buffered tablet were purchased from Sigma-Aldrich, USA. Triethylamine was purchased from Merck, USA. Cell culture reagents were obtained from Gibco, UK. COX-1/COX-2 enzyme assay kit was purchased from Cayman Chemical, USA. TNF- α assay kit was obtained from Elabscience, USA. All used materials were pharmaceutical grade.

Preparation of Thermosensitive Hydrogels

Thermosensitive hydrogels were prepared using P188, P407, and HPMC by the cold method in line with previous studies with some modifications [17, 28]. Initially, poloxamers were added to a beaker containing a required amount of chilled distilled water (4–8°C), and the beaker was stirred in a cold-water bath (4 \pm 1°C) placed on a magnetic stirrer at 300 rpm for 2 h. The homogenized solution was waited for 1 h to reach room temperature (RT). Subsequently, HPMC was added to the poloxamer solution, and the solution was stirred at 300 rpm for 1 h. Finally, benzalkonium chloride (0.02%, w/w) was added, and the hydrogel was stirred until homogeneous. In the context of preliminary studies, 33 formulations without BZD (16–20%, P407; 0–12%, P188; 0–0.5%, HPMC) were prepared, and lead formulations were selected in terms of the results of viscosity (at 25°C) and gelation temperature studies. Drug-containing formulations were prepared as abovementioned; in the last stage, BZD (5%) was added to the solution and stirred at RT until BZD dissolved. The amounts of the components (weight/weight (w/w)) are demonstrated in Table I.

Characterization of Thermosensitive Hydrogels

To characterize the formulations and to determine the lead formulations for topical application, physicochemical

Table 1 Composition and Physicochemical Characterization of BZD-Containing Thermoinsensitive Hydrogel Formulations (n = 3)

Formulation	BZD (% w/w)	P407 (% w/w)	P188 (% w/w)	HPMC K4M (% w/w)	Benzalkonium chloride (% w/w)	Distilled water (% up to 100, w/w)	pH (± SD)	Gelation temperature (°C ± SD)	Spreadability (cm ± SD)	Gelation capacity	Clarity	Content uniformity (% ± SD)
F11	5	18	-	0.25	0.02	100	5.74 ± 0.01	33.7 ± 0.46	6.53 ± 0.14	+++	++	100.67 ± 2.64
F15	5	18	9	0.5	0.02	100	5.77 ± 0.02	31.0 ± 1.22	9.38 ± 0.09	+++	+	102.11 ± 5.77
F16	5	18	12	-	0.02	100	5.94 ± 0.03	33.0 ± 1.63	9.70 ± 0.09	+++	+++	99.63 ± 4.43
F17	5	18	12	0.25	0.02	100	5.87 ± 0.03	31.0 ± 2.34	9.03 ± 0.12	+++	++	107.25 ± 3.02
F18	5	18	12	0.5	0.02	100	5.90 ± 0.02	28.0 ± 2.12	8.73 ± 0.08	+++	+	100.70 ± 1.64
F19	5	20	-	-	0.02	100	5.76 ± 0.01	32.8 ± 0.55	6.23 ± 0.13	+++	+++	97.16 ± 0.90
F20	5	20	-	0.25	0.02	100	5.75 ± 0.01	29.9 ± 0.79	6.13 ± 0.19	+++	+++	105.64 ± 1.84
F21	5	20	-	0.5	0.02	100	5.77 ± 0.01	28.9 ± 1.25	5.90 ± 0.11	+++	++	105.23 ± 1.37
F23	5	20	6	0.25	0.02	100	5.97 ± 0.00	30.7 ± 2.27	6.10 ± 0.22	+++	++	102.11 ± 5.77
F32	5	20	9	0.25	0.02	100	5.81 ± 0.03	26.3 ± 4.96	6.21 ± 0.17	+++	++	94.84 ± 2.19

properties of the formulations including those on appearance, gelation temperature, gelling capacity, viscosity, pH, spreadability, sprayability, and content uniformity were investigated at least in triplicate.

Appearance

Hydrogels in a transparent beaker were visually examined on both dark and white backgrounds in terms of turbidity, color, clarity, and whether they had a particle. The visual assessment was graded as follows: very clear (+++), clear (++), and blurred (+) [12].

Gelation Temperature (T_{sol-gel})

Accurately weighed 10 g of hydrogel (4–8°C) was transferred to a beaker. The beaker was stirred on a magnetic heating stirrer (RT 15, IKA, Germany) at 200 rpm. A digital thermometer was immersed in the beaker, and the temperature of the stirrer was raised 2°C per min. The temperature at which the magnetic bar stopped due to gelation was noted as the gelation temperature. The studies were carried out until 45°C [29].

Viscosity

The viscosity of the formulations was individually measured with a rotational viscometer (DV2T-RV, Brookfield, USA) at 4 ± 1, 25 ± 1 and 32 ± 1°C. The temperature was fixed using a circulating water bath (Alpha RA 8, Lauda, Germany). The required amount of formulation was transferred to a metallic tube, and the measurement was performed using a cylindrical spindle (SC21).

pH

To determine the pH of the hydrogels, a probe of pH meter (HI83141, Hanna Instruments, USA) was immersed in the gel and waited until the value was constant. The measurements were repeated three times by immersing the probe in the different parts of the gel. The mean value was assessed as the pH of the gel.

Gelling Capacity

The studies were performed according to previous studies with minor modifications [12, 30]. One drop of the formulation was added to a beaker containing 5 mL of distilled water at 32–34°C, and time was tracked by holding a stopwatch. The gelling capacity of the formulations was followed visually. The fact that the dropped formulation remained in the form of a droplet without dispersing in the water was considered an indication of gelation and the gelling time was

noted. The gelling capacity was evaluated based on the result of the gelling time as follows: immediate (a few seconds) gelation (+++).

Spreadability

The formulation taken from the refrigerator was kept at RT for at least 1 h, and then 1 g of the formulation weighed into the center of a glass plate ($20 \times 20 \text{ cm}^2$) heated at $32 \pm 2^\circ\text{C}$. The plate was placed onto a hot plate ($32 \pm 2^\circ\text{C}$) and was compressed using the same size of a glass plate. After 1 min, the diameter of the spread area was measured with a ruler [31].

Sprayability

To evaluate the sprayability of the formulations, a novel method was designed and developed. A texture analyzer (TA.XTplusC, Stable Micro Systems, Haslemere, Surrey, UK) was used to perform an equal force during each process. First, a certain amount of blue dyestuff (E133) was added to each formulation and mixed. The hydrogel was transferred to a spray bottle (20 mL of volume, polyethylene). The bottle was placed under a probe (SPS P 35, $\varnothing = 35 \text{ mm}$) of the texture analyzer, and a white paper plate was placed vertically at a distance of 20 cm from the bottle (Fig. 2a). The probe was moved at 30 mm/s by pressing the down button of the device, and spraying was performed. Finally, the diameter of the spray area was measured with a ruler. Also, it was visually detected whether there was any gel leak on the nozzle of the bottle. Moreover, to determine the weight of a single spray application, each hydrogel was sprayed into a beaker and weighed after each process. The studies were performed five times for each batch.

Content Uniformity

A gel of 0.1 g was individually taken from different points of the containers containing BZD-loaded formulations and transferred to a beaker. A mobile phase (35:65 of ACN:water) of 100 mL was added to the beaker and stirred at 500 rpm for 1 h. One milliliter was taken and filtered using a membrane filter (0.22 μm , cellulose acetate (CA), Merck Millipore, USA). The samples were analyzed by HPLC at 308 nm. The study was performed in 4 repetitions for each batch.

An HPLC method was developed and validated to quantify the amount of BZD in the samples of content uniformity, *in vitro* drug release, and *ex vivo* permeability studies. HPLC device (Agilent 1100 series, USA) equipped with a UV detector was used, and the parameters were set to 20 μL of injection volume, 1 mL min^{-1} of flow rate, 308 nm of wavelength, and 25°C of column temperature. Acetonitrile

and pH 3 phosphate buffer including 0.5% triethylamine (pH 3 adjusted by o-phosphoric acid) (35:65, v/v) were used as a mobile phase [32]. BZD solutions (10–250 $\mu\text{g}/\text{mL}$) were analyzed using a C18 column (5 μm , $150 \times 4.6 \text{ mm}$, Inert-Sustain, GL Sciences, Japan). The device was conditioned with the mobile phase for at least 45 min. Precision, recovery, reproducibility, limit of detection (LOD), and limit of quantification (LOQ) parameters were studied to validate the developing method according to ICH guideline [33].

Bioadhesion Studies

Ex vivo bioadhesion studies were carried out using a Balb/c mice skin by the texture analyzer to compare the bioadhesive properties of the formulations as in the previous study with some modification (Fig. 3a, b) [34, 35]. The shaved skin was fixed to a cylindrical probe (Perspex SNSP/10, θ : 10 mm) using an elastic band. One gram of gel was transferred to a beaker. The beaker was adhered to a heating device using double-sided tape. While the pre-test speed was adjusted to 0.5 mm/s, the test and post-test speeds were 0.1 mm/s. The contact time was set as 120 s. The highest force during the separation of the skin from the gel was recorded as the bioadhesive force. The area under the curve (AUC_{1-2}) obtained from a force-distance plot was determined using the software program, and the work of adhesion was calculated with the following equation (Eq. 1). The experiments were performed at $34 \pm 1^\circ\text{C}$.

$$\text{Work of adhesion (mJcm}^{-2}\text{)} = \text{AUC}_{1-2} / \pi r^2 \quad (1)$$

πr^2 : the area of the skin being in contact with the gel.

Drug Release Studies

The dialysis bag method was used to perform drug release studies of BZD-containing *in situ* formulations. A total of 500 mg of the formulation was individually weighed into a dialysis bag (molecular weight cutoff: MCWO 12–14 kDa), and the mouth of the bag was closed tightly using magnetic closures. pH 7.4 phosphate buffer (200 mL) was filled into a beaker. The study was carried out on a digital magnetic hotplate stirrer (RT 15, IKA, Germany) at 50 rpm and $34 \pm 1^\circ\text{C}$ [12]. As soon as the dialysis bag was immersed into the medium, the mouth of the beaker was closed with parafilm to keep the temperature constant. At the time intervals (0.25, 0.5, 0.75, 1, 1.5, 2, 3, 4, 6, 8, 10, 12 h), one mL of sample was taken and filtered using a membrane filter (0.22 μm , CA) and replaced with the equal volume of fresh medium. The samples were analyzed by HPLC at 308 nm.

On the one hand, to assess the release data of the formulations, model-dependent methods including Higuchi, Hixson-Crowell kinetic models, and Korsmeyer-Peppas equation

were applied [36]. On the other hand, model-independent methods including difference factor (f_1) and similarity factor (f_2) were utilized [37, 38] to evaluate the BZD release profiles.

Ex Vivo Permeation and Penetration Studies

The experiments of the study were carried out in line with National Institutes of Health (NIH) guidelines. A shaved abdominal skin extracted from Balb/c mice in accordance with the rules of Istanbul Medipol University Ethical Council (approval no: 10.01.2022-07) was used in the bioadhesion and *ex vivo* permeability studies. The studies were performed using a Franz diffusion cell system having a volume of acceptor compartment of 12 mL and a diffusion area of 1.77 cm². The skin (2 × 2 cm²) was thawed at least 30 min before starting the experiments. The acceptor compartment was filled with a buffer solution (pH 7.4). The skin was tautly placed between the acceptor and donor compartment using a metal clamp. The experiments were carried out under continuous stirring (300 rpm) at 37 ± 2°C for 24 h. A sample of 0.5 mL was taken and filtered, then replaced with an equal volume of the buffer solution [39]. The cumulative amount of drug permeated over 24 h was determined from the data obtained by HPLC analysis. Moreover, flux (J_{ss}), permeability coefficient (K_p), and lag time of the formulations were calculated using the permeation data obtained [40].

At the end of the study, the skin was cut into small pieces and transferred to a tube including 10 mL of ACN:water (35:65). The tube was vortexed for 5 min, stirred 1 h on a magnetic stirrer, and centrifuged (3–18 KS, Sigma, USA) at 14,000 rpm for 30 min. A sample of 1 mL was taken from the supernatant and analyzed by HPLC device.

Cytotoxicity Assay

Human embryonic kidney cell line HEK293 (CRL-1573, ATCC) was grown in Dulbecco's Modified Eagle's Medium/high glucose (DMEM/High) supplemented with 10% (v/v)

heat-inactivated fetal bovine serum, L-glutamine (2 mM), and antibiotic-antimycotics solution (100 U/mL penicillin, 100 µg/mL streptomycin, and 0.25 µg/mL amphotericin B) at 37°C in a humidified incubator containing 5% CO₂. The cells were passaged every 3 days. Cell viability was determined using the MTT assay as described. Cells were cultured in a flat-bottomed 96-well plate at a density of 1 × 10⁵ per well 24 h prior to treatment. For detecting the cytotoxic activity of formulations, the cells were treated with increasing concentrations of the formulations diluted with DMEM/High (0.1–1000 µg/mL). After the treatment, the medium was removed and replaced by 30 µL of the MTT (0.5 mg/mL in sterile D-PBS) solution per well, and the plates were incubated for 4 h. Then, 150 µL of isopropanol was added to each well to dissolve the formazan crystals, and the absorbance of formazan products was measured at 570 nm in a microplate reader (SpectraMax i3, USA). Formulations were analyzed at least in triplicate in three independent assays, and viability (%) was calculated with the equation (Eq. 2) below [41].

$$\text{Viability (\%)} = \frac{[\text{absorbance}_{\text{treated}}]/[\text{absorbance}_{\text{control}}]}{1} \times 100 \quad (2)$$

COX-1/COX-2 Enzyme Assay

The formulations were tested using a commercial COX-1 (ovine), COX-2 (human recombinant), fluorometric inhibitory screening assay kit following the instructions recommended by the manufacturer (Cayman test kit 700100, Cayman Chemical Company, Ann Arbor, MI, USA). Initially, 150 µL of assay buffer (0.1 M Tris-HCl pH 8.0), 10 µL of heme, 10 µL of enzyme (COX-1 or COX-2), and 10 µL of the compounds to be tested were added to the wells. After 5 min at RT, 10 µL of ADHP (10-acetyl-3 7-dihydroxyphenoxazine) and 10 µL of arachidonic acid were added to start the reaction. The plate was incubated at RT for 2 min. After, fluorescence was measured at 530 nm (excitation) and 585 nm (emission) [42]. Stock solutions of the formulations were prepared with below 1% of DMSO. The data were expressed as mean ± standard deviation (SD). Inhibition (%) was calculated with the equation (Eq. 3) below.

$$\text{Inhibition (\%)} = \frac{[(\text{initial activity} - \text{sample activity})/\text{initial activity}]}{1} \times 100 \quad (3)$$

TNF-α Assay

The concentrations of TNF-α were measured using specific ELISA kits according to the manufacturer's instructions (Elabscience, USA, and EIAab, China).

HEK293 cells were incubated in 96-well plates for 24 h at 37°C in 5% CO₂. After the formulations at (selected non-toxic concentration) treatment for 48 h of the cells, a brief centrifugation step at 2000×g was applied to remove dead cells and cell debris, and the supernatants were subjected to ELISAs [43].

Statistical Analyses

The data were demonstrated as mean \pm SD. Statistical analyses were performed using a software program (version 9.0.1., GraphPad Prism, CA, USA). To evaluate statistically significant discrepancies, one-way analysis of variance (ANOVA) was utilized between three or more groups. Besides, Tukey's multiple comparisons test was applied. $p < 0.05$ was admitted as statistically significant.

Results and Discussion

Thermosensitive drug delivery systems offer unique opportunities for topical application due to their advantages such as reducing dose frequency or amount and increasing patient compliance [9]. Apart from poloxamers, which are most frequently preferred in the preparation of thermosensitive gels, lots of natural and synthetic polymers such as HPMC, polyvinylpyrrolidone, sodium carboxymethyl cellulose, chitosan, Carbopol, and xanthan gum are used thanks to bioadhesive ability, sol-gel transition properties, and/or capability of increasing mechanical strength [23, 28, 44, 45]. In this project, HPMC, which could provide all the advantages, was employed, and its effect on characterization of the formulations was revealed.

Within the scope of preliminary studies, BZD-free and BZD-containing formulations were prepared, and the viscosity at RT and the gelation temperature were investigated. At the end of the preliminary studies, it was determined that the formulations with a gelation temperature between 26 and 34°C and a viscosity at RT lower than around 300 mPa·s were lead hydrogels in order to ensure that the formulations could be easily sprayed [46–50].

Characterization of Thermosensitive Hydrogels

The characterization studies of ten lead formulations selected with referencing two main properties abovementioned were performed. The clarity, pH, gelation temperature, and viscosity (at RT) of BZD-free formulations and the clarity, pH, gelation temperature, gelling capacity, spreadability, viscosity, sprayability, and content uniformity of BZD-containing formulations were determined, and the effect of BZD addition on these physicochemical properties was investigated.

Clarity and Gelling Capacity

The clarity of drug-free and drug-containing formulations was similar. The formulations that incorporated high amounts of HPMC were more blurred. This situation was

more evident when formulations were stored at 4°C. The appearance of the formulations was usually evaluated to be satisfactory (Table I). Also, the gelling capacity of the formulations was good because one drop sol underwent gelation as soon as dropped into distilled water [51, 52].

pH

The pH of topical formulations should be compatible with skin pH, which is normally acidic ranging from 4 to 6 in order to not cause irritation and allergic conditions [53]. The pH of BZD-containing formulations was found between 5.74 and 5.97 (Table I). The addition of BZD to the formulations did not cause a significant change in pH values ($p > 0.05$, data not shown). It was assessed that the pH of formulations was appropriate for the skin pH.

Gelation Temperature

Thermosensitive formulation administered to the skin should immediately turn into gel from sol form with the body temperature. It can be considered appropriate that the gelation temperature of thermosensitive hydrogels for topical delivery is generally between 26 and 34°C [12, 28, 48, 54, 55]. In the light of literature, BZD-containing hydrogels were suitable for topical application (Table I). Generally, while the gelation temperature decreased with an increase in the amount of P407 and HPMC, it increased with the addition of P188 in low amounts but decreased when P188 was employed in high amounts.

The triblock structure of poloxamers in the form of PEO-PPO-PEO enables them to present different physical characteristics with changing temperatures. At a low temperature, hydrogen bonds dominate between hydrophilic ethylene oxide chains and water, and the system behaves like a liquid, while hydrophobic interactions increase depending on the temperature increase, leading to dehydration and conformational changes in the hydrophobic chain regions, increasing the chain friction and the entanglement of the polymeric network. As a result, spherical micellar structures formed by hydrophilic PEO outwardly and hydrophobic PPO chains inwardly occur. Therefore, at the critical micelle concentration, there is more unbound water in the hydrophilic regions of the gel, and gelation occurs at this point as the outer PEO chains are densely intertwined in the gel [20, 56]. As P188 is more hydrophilic than P407, the gelation temperature increases with the addition of a small amount of P188 in the formulation due to the change in PEO proportion. However, the use of a high amount of P188 causes the development of additional micelles that contribute to the formation of gel in blend solutions. For this reason, increasing P188 concentration induces a decrease in gelation temperature after

Table II Gelation Temperature and Viscosity (at 25 ± 1°C) of BZD-Free and BZD-Containing Thermosensitive Formulations (n = 3)

Formulation		Gelation temperature (°C ± SD)	Viscosity at 25 ± 1°C (mPa·s ± SD)
F11	BZD (-)	19.9 ± 0.27	ns*
	BZD (+)	33.7 ± 0.46	80.5 ± 8.7
F15	BZD (-)	28.5 ± 1.12	262.0 ± 4.0
	BZD (+)	31.0 ± 1.22	212.0 ± 20.7
F16	BZD (-)	31.6 ± 1.55	181.0 ± 7.1
	BZD (+)	33.0 ± 1.63	201.0 ± 31.9
F17	BZD (-)	29.8 ± 2.20	247.5 ± 5.0
	BZD (+)	31.0 ± 2.34	248.5 ± 34.1
F18	BZD (-)	27.8 ± 2.09	280.0 ± 4.0
	BZD (+)	28.0 ± 2.12	286.5 ± 37.5
F19	BZD (-)	20.2 ± 0.34	ns*
	BZD (+)	32.8 ± 0.55	101.0 ± 6.6
F20	BZD (-)	18.9 ± 0.50	ns*
	BZD (+)	29.9 ± 0.79	143.0 ± 12.4
F21	BZD (-)	18.3 ± 0.83	ns*
	BZD (+)	28.9 ± 1.25	184.5 ± 16.9
F23	BZD (-)	22.6 ± 1.67	ns*
	BZD (+)	30.7 ± 2.27	240.5 ± 20.5
F32	BZD (-)	22.5 ± 4.19	ns*
	BZD (+)	26.3 ± 4.96	293.5 ± 22.7

* > 2500 mPa·s, BZD (-): BZD free, BZD (+): BZD containing ns not specified

a certain concentration [57]. As seen in Tables I and II, our findings were compatible with the literature.

Furthermore, the addition of BZD usually caused a significant increase in the gelation temperature of the formulations (Table II, p < 0.05). However, it was not significant for formulations (F16, F17, and F18) having the highest poloxamer concentration (p > 0.05). The differences between the

gelation temperatures of BZD-free and BZD-containing formulations of F20, F23, and F32 containing the same amount of HPMC and P407 were 11, 8.1, and 3.8°C, respectively. According to these results, it was found that the rate of increase in gelation temperature, which emerged with the addition of BZD, decreased with increasing P188 amount. These results may be related to increased total poloxamer concentration or P188 alone.

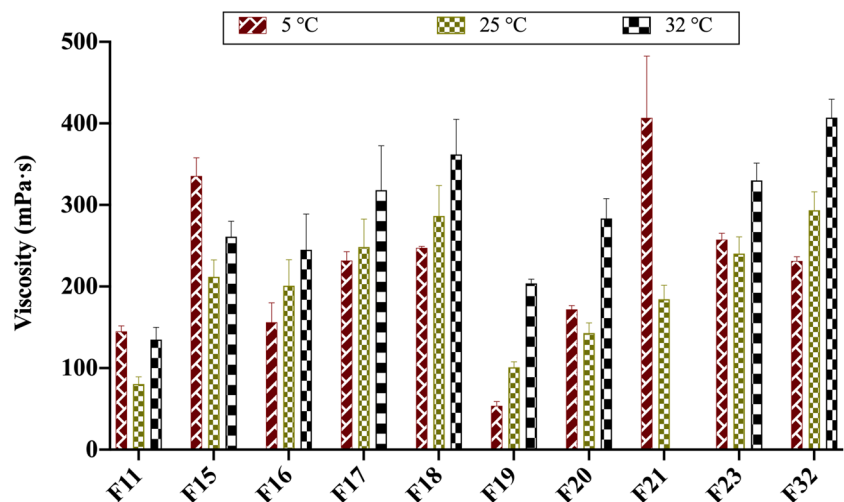
Akkari *et al.* [58] showed that ropivacaine (0.5%) added to thermosensitive formulations containing P188 and P407 increased the gelation temperature. Gholizadeh *et al.* [10] stated that in the preparation of chitosan-based thermosensitive gels containing tranexamic acid (0.1–2%), gelation temperature was increased when the active substance was added at high concentrations. The results were compatible with the mentioned literature. The increase in gelation temperature resulting from the addition of the high amount of BZD may be associated with reducing interactions between polymer chains.

Viscosity and Spreadability

The viscosity of formulations is critical for their sprayability. The aim is that the viscosity of the formulations at RT is at a value that allows them to be sprayed easily. The viscosity of BZD-containing formulations is presented in Fig. 1. The viscosity mostly increased with increasing HPMC concentration at all temperatures. For the formulations without P188, the viscosities of the formulations were generally listed as follows: FX_{32°C} > FX_{5°C} > FX_{25°C}. The viscosity increased with increasing total poloxamer concentration.

The effect of BZD on the viscosity of the formulations was assessed by measuring the viscosity at RT (Table II). BZD decreased the viscosity for all formulations except F16. Since BZD weakened separately the interchain bonding of poloxamer and HPMC, it induced a decrease in the

Fig. 1 Results of viscosity at different temperatures of BZD-containing thermosensitive formulations (n = 3)



viscosity values at RT while increasing the gelation temperature. It was observed that this change was less with increasing HPMC, P188, and P407 concentrations. The addition of BZD did not significantly affect the viscosity of F16, F17, and F18 incorporated the highest poloxamer amount ($p > 0.05$). These data were compatible with the change in gelation temperature. A viscosity of less than 300 mPa·s is required for formulations to be sprayed at RT [46, 47]. Therefore, formulations with the lowest viscosity were more appropriate. The spreadability of thermosensitive formulations was found between 5.90 and 9.70 cm (Table I). The results indicated that viscosity and spreadability were inversely proportional and the data were consistent with the literature [39].

Content Uniformity

The correlation coefficient and the equation of developing the HPLC method were found to be 0.9999 and $y = 19.1770x + 7.3579$, respectively. LOD and LOQ of BZD were calculated as 0.017 ± 0.003 and 0.052 ± 0.009 $\mu\text{g/mL}$, respectively. The variation coefficient of all validation parameters was found to be lower than 2%, and the method was assessed as having a high precision and reproducible for the quantification of BZD. The content uniformity of thermosensitive gels was found between 94.84 and 107.25% (Table I).

Sprayability

Thermosensitive hydrogels are in liquid form at 4–8°C and can generally be sprayed easily. However, a product taken

from the refrigerator and applied directly to the body causes an important disadvantage in terms of patient compliance due to its cold feeling, as well as creating costs and difficulties in terms of storage. For this reason, it was aimed that the developed formulations could be sprayed at RT. The sprayability of hydrogels was investigated by a novel method designed and developed by our group using a texture analyzer. The diameter of the spray area of the formulations was found to be between 2.3 and 7.6 mm (Fig. 2d), while the weight of a single spray application ranged from 66 to 155.6 mg (Fig. 2e). The diameter of the spray area was low. However, the main purpose was not to spread the formulation in sol form over a wide area by spraying but to deliver it to the skin without any gel leak on the spray nozzle of the bottle. The sprayability of gels having lower viscosity was better than the gels with higher viscosity. Namely, the sprayability of the formulations was inverse to their viscosity. The most easily sprayable formulations were F11, F19, F20, and F21 which had the lowest viscosity at RT, and no leak was found on the nozzle during spraying studies of these formulations (Fig. 2b). Similar results were found for the F15 formulation. However, while the nozzle of F23 and F32 was individually congested after a couple of spraying processes (Fig. 2c), a leak of the gel occurred on the nozzle during the spraying process of F17 and F18.

Wong *et al.* [14] investigated the viscosity and sprayability properties of thermosensitive gels containing P407 and HPMC/sodium alginate. They showed that formulations with viscosity values of 100–180 mPa·s at RT can be easily sprayed. In another study, it was revealed that a nasal *in situ* gel with 150 mPa·s at RT showed a sprayability profile similar to the solution of the active substance [10]. Evidently, the

Fig. 2 **a** The image of sprayability studies performed using a texture analyzer. **b** During the spraying process of the F11, F19, F20, and F21, there was no residue or clogging in the spray nozzle. **c** In the spraying process of F23 and F32, spraying did not occur as desired, some gel remained in the nozzle. **d** Results of spreading diameter after spraying process. **e** The weight of sprayed gel after per spraying process (n=5)

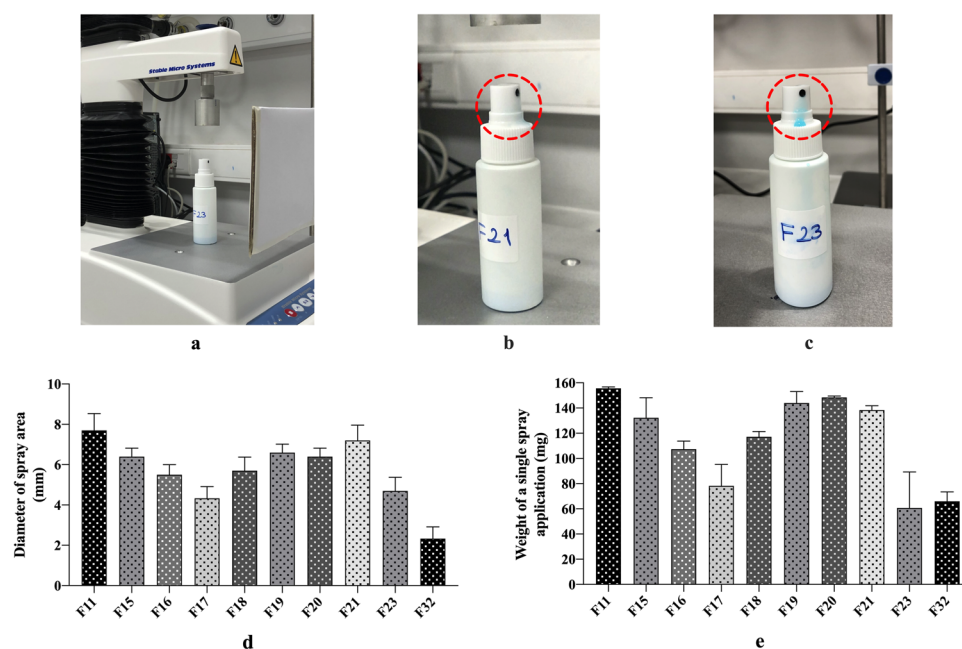
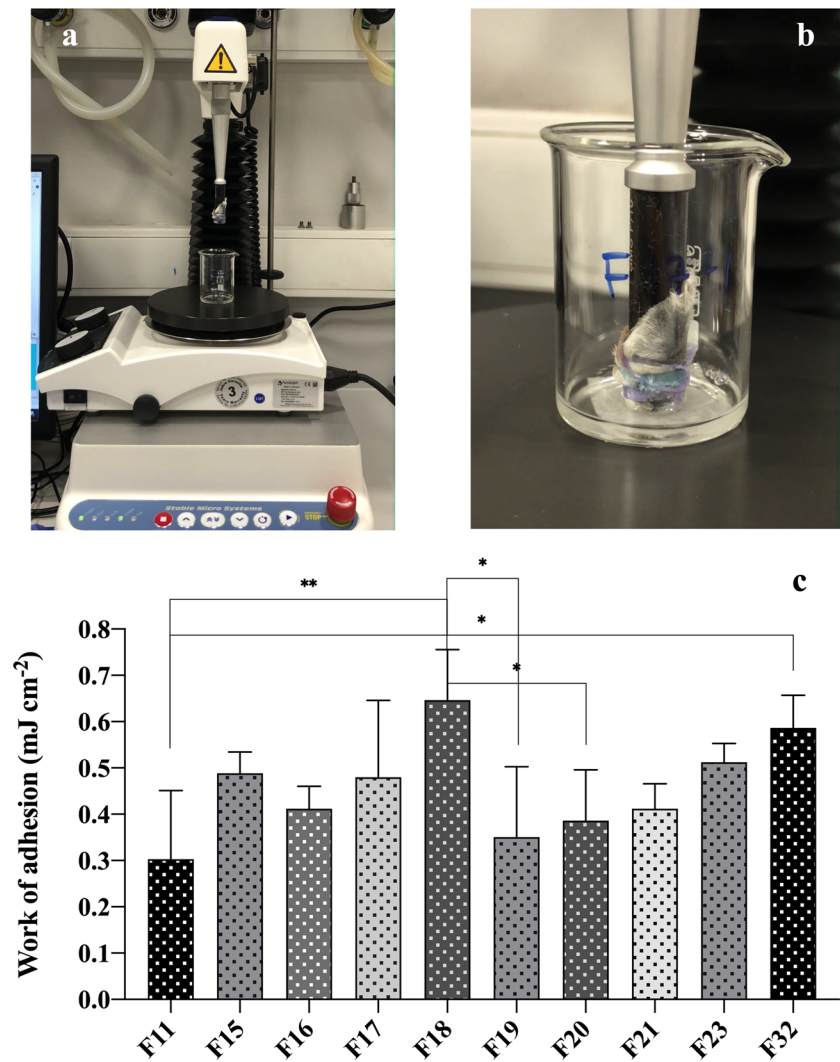


Fig. 3 **a** *Ex vivo* bioadhesion study design performed using a Balb/c mice skin by the texture analyzer. **b** Close-up image of hydrogel and tissue contact. The skin was fixed to the probe with an elastic band, and the beaker containing the hydrogel was attached to the heating plate with double-sided tape. **c** Findings of bioadhesion studies carried out using a Balb/c mice skin in a texture analyzer. (* indicates a significant difference, * $p < 0.05$, ** $p < 0.01$) ($n = 4$)



spraying studies revealed that the viscosity at RT of thermosensitive formulations should be lower than around 200 mPa·s to spray easily.

Bioadhesive Properties

The results of bioadhesion studies are demonstrated in Fig. 3c. The formulations having the highest and the lowest bioadhesive capability were F18 and F11, respectively ($p < 0.01$). In general, increasing total poloxamer and HPMC amounts positively affected bioadhesive properties. However, the effect of HPMC on the bioadhesive character of the formulation was not statistically significant ($p > 0.05$). This may be related to the very small change in HPMC concentration. Baloğlu *et al.* [18] stated that the increase of P407 improved the adhesivity in their study investigated the effect of a poloxamer mixture on the rheological and mechanical properties of a mucoadhesive gel base. The PEO segment of P407 contributed to improving the

bioadhesive ability of the semi-solid formulations; thus as the P407 amount was increased, the bioadhesion improved [59]. In another study, thermostable gels of metoprolol succinate were developed using HPMC and P407. The bioadhesive strength increased with the increase of both HPMC and P407 [60]. Choi *et al.* [61] reported a significant increase in the bioadhesive strength of the thermosensitive liquid suppository with increasing P188 concentration, while the amount of P407 was constant. Thus, the mentioned literature supported the obtained data.

Drug Release Studies

Viscosity, sprayability, and gelation temperature were the main criteria for the selection of ideal formulations. The formulations with good sprayability, a viscosity at RT of lower than 200 mPa·s, and a gelation temperature of under 34°C were determined as lead formulations. As a result, F11, F15, F19, F20, and F21 were selected for drug release studies.

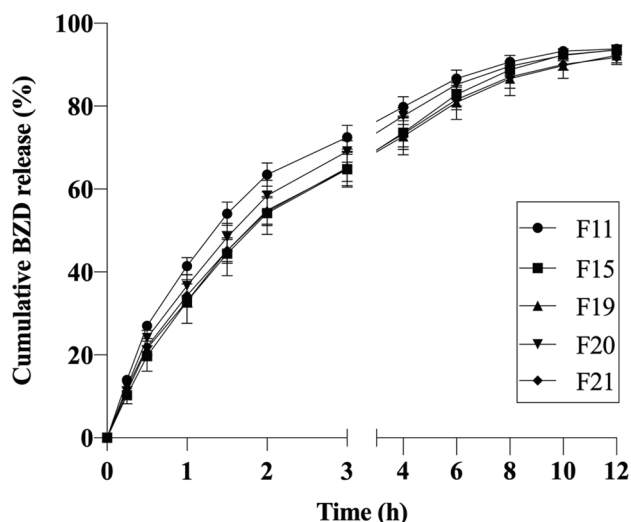


Fig. 4 Cumulative BZD release from thermosensitive formulations using a dialysis bag method at 34°C (n = 4)

Although drug release studies of topical formulations are usually performed at 32°C and pH 5.5 of release medium mimicking the natural skin conditions, instead, the studies were carried out at 34°C to ensure that all formulations transition from sol to absolute gel form [12]. Also, to simulate *in vivo* absorption process, it was used pH 7.4 phosphate buffer as a release medium, based on the previous studies [12, 62, 63].

According to the results of drug release studies, cumulative BZD release reached 60–70% within 3 h, and it reached approximately 100% at the end of 12 h (Fig. 4). Since BZD-containing thermosensitive formulations in the dialysis bag gelled as soon as it was immersed into the release medium, the drug release continued for about 10–12 h. The release profile of BZD-containing formulations was investigated using Higuchi and Hixson-Crowell kinetics (Table III). The kinetic model with the highest correlation coefficient was accepted as the most appropriate kinetic. Higuchi kinetic showed the best fit kinetic for all formulations. Higuchi kinetics is the first mathematical model aimed at defining the release of water-soluble active ingredients from a matrix system [64]. According to Higuchi kinetic, cumulative drug release concentration

is associated with the square root of time, and the release of the drug from the formulation, which is homogeneously dispersed throughout the hydrogel matrix, occurs via diffusion and/or matrix dissolution or erosion [26, 36, 65]. Sathyanarayana *et al.* [66] reported that Higuchi kinetic had the highest kinetic constant for release data of Bimatoprost-loaded P407/P188 and HPMC-based *in situ* gels. In another study, the data of metronidazole release from P407 and methyl cellulose-based hydrogels were compatible with Higuchi kinetic which showed the highest constant, indicating that metronidazole release occurred with the diffusion controlled [67]. The release data of up to 70% of cumulative BZD releases were applied to the Korsmeyer-Peppas model. The r^2 values of all formulations were found to be around 0.99, while n values were between 0.6835 and 0.7113. A value of n between 0.5 and 1 indicates diffusion and non-Fickian (anomalous transport) release. These findings showed that BZD release from thermosensitive formulations was time-independent and the drug release was diffusion and erosion controlled [68–71]. The data obtained was consistent with the literature.

Again, model-independent kinetic models were applied to examine the similarity between the BZD release

Table IV Model-Independent Kinetics Between BZD-Containing Thermosensitive Formulation Pairs

Formulation pair	Model-independent kinetics	
	f1 (difference factor)	f2 (similarity factor)
F11 – F19	10	59
F11 – F20	5	73
F11 – F21	9	60
F11 – F15	9	59
F15 – F19	2	88
F15 – F20	5	73
F15 – F21	2	88
F19 – F20	6	72
F19 – F21	1	96
F20 – F21	5	75

Table III Kinetic Data of BZD Release Profile from Thermosensitive Formulations

Formulation	Higuchi		Hixson-Crowell		Korsmeyer-Peppas	
	(r^2)	k	(r^2)	k	(r^2)	n
F11	0.8811	26.004	0.6090	0.1556	0.9891	0.7172
F15	0.9272	27.248	0.6659	0.1736	0.9883	0.7495
F19	0.9313	28.533	0.6687	0.1783	0.9902	0.7113
F20	0.9069	27.210	0.6414	0.1674	0.9859	0.6908
F21	0.9266	27.035	0.6698	0.1761	0.9914	0.6835

characteristics of the formulations. Among all formulation pairs, the f_1 -difference factor was less than 15, while the f_2 -similarity factor was greater than 50 (Table IV). These values are the reference to admit the similarity between the release profiles [38]. The results proved that the release profiles in Fig. 4 were similar. Increasing HPMC concentration did not almost any difference in the release profile of BZD, while increasing P407 and P188 concentrations affected in drug release profile; however, it was not statistically meaningful ($p > 0.05$).

Ex Vivo Permeation and Penetration Studies

It is intended that the applied formulation undergoes gel at the body temperature and is localized in the skin without entering the systemic circulation. BZD permeated through the skin was determined to be quite low (36.52–64.01 $\mu\text{g}\cdot\text{cm}^{-2}$) (Fig. 5a), while the amount of BZD accumulated in the skin was found to be between 578.69 and 995.59 $\mu\text{g}\cdot\text{cm}^{-2}$ (Fig. 5c). Permeability parameters such as flux, permeability coefficient, and lag time are shown in Fig. 5b. While the flux representing the amount of drug passed through a unit area (1 cm^2) depending on time [72] was between 1.587 and 2.928 $\mu\text{g}\cdot\text{cm}^{-2}\cdot\text{h}^{-1}$, the lag time defined as the time required for the diffusion of the drug to reach a steady state [73] ranged from 1.131 to 1.623 h. Compared to the other formulations, F11 had a higher flux and permeability coefficient and lower lag time. Increasing poloxamer concentration appeared to have a positive effect on the skin penetration of BZD. However, it was understood that the increased viscosity of the formulation also has a negative effect on skin penetration. The higher permeability and penetration of F11 compared to F21, although there was not much difference in terms of the contents of the formulations, could be associated with the lower viscosity properties of F11 ($p < 0.05$). The similar penetration ability between F11 and F15

(which had a higher viscosity than F11) might be due to the higher HPMC and P188 concentration of F15 ($p < 0.05$). Likewise, although F15 and F21 presented very similar drug release profiles, F15 exhibited higher penetration properties. These findings can also be interpreted as higher poloxamer concentration increases the permeability. On the one hand, Latif *et al.* [74] reported an increase in flux and permeability of methotrexate due to increased HPMC concentrations in *ex vivo* permeation studies for patch formulations. It was also found that the formulation containing the highest concentration of HPMC penetrated the deeper layers of the skin. On the other hand, in another study where HPMC (1–3%) was used as a gel-forming agent, it was observed that the viscosity of the formulation increased significantly due to the increased amount of HPMC, and accordingly, the penetration depth decreased because the diffusion of the active ingredient from the formulation became difficult [75]. Therefore, it can be concluded that HPMC has penetration-enhancing abilities but can reduce penetration when it increases viscosity significantly in semi-solid formulations.

Although BZD, which can be administrated both locally and systemically, is well absorbed by oral administration, it shows poor absorption in the administration of mouthwash, dermal cream, and vaginal douche. In other words, it is known that the amount of drug accumulated in the tissue is higher in the topical application than in the oral application and the systemic effect is less when the drug is administrated through the skin and non-specified mucous membranes [6]. Besides, due to its alkaline pH, BZD selectively accumulates in the inflamed tissue and stabilizes the microvasculature, thus minimizing the harmful effect of inflammatory substances [7]. As highlighted in the previous studies, the accumulation of BZD in the tissue/mucosa and as a result of topical application can be considered an important advantage in the treatment of diseases such as inflamed joints.

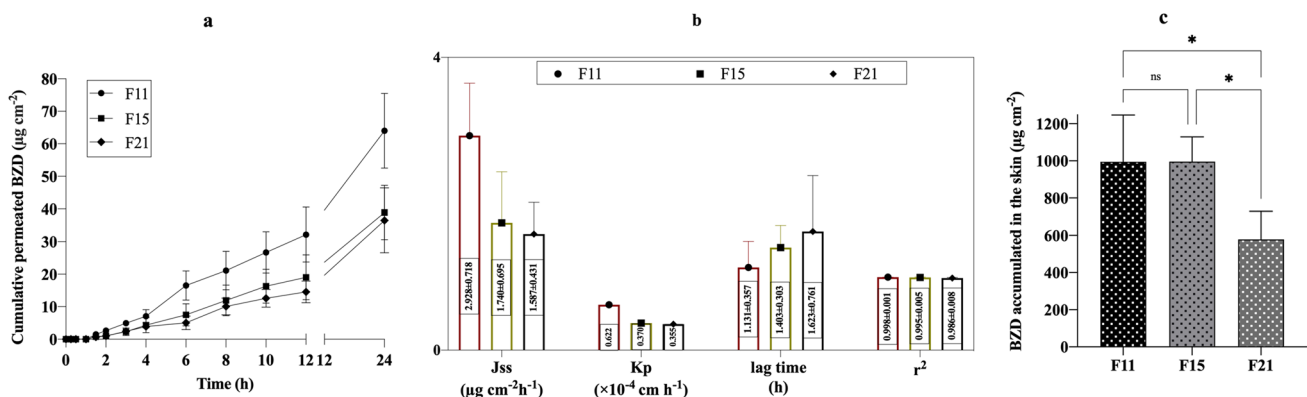


Fig. 5 Results of *ex vivo* permeability and penetration study using a Balb/c mice skin by Franz diffusion cell ($n = 4$). **a** The graph represents cumulative permeated BZD through the skin. **b** The permea-

tion parameters of BZD-containing thermosensitive hydrogels. **c** The graph represents BZD accumulated in the skin at the end of 24 h. (* indicates a significant difference, $*p < 0.05$)

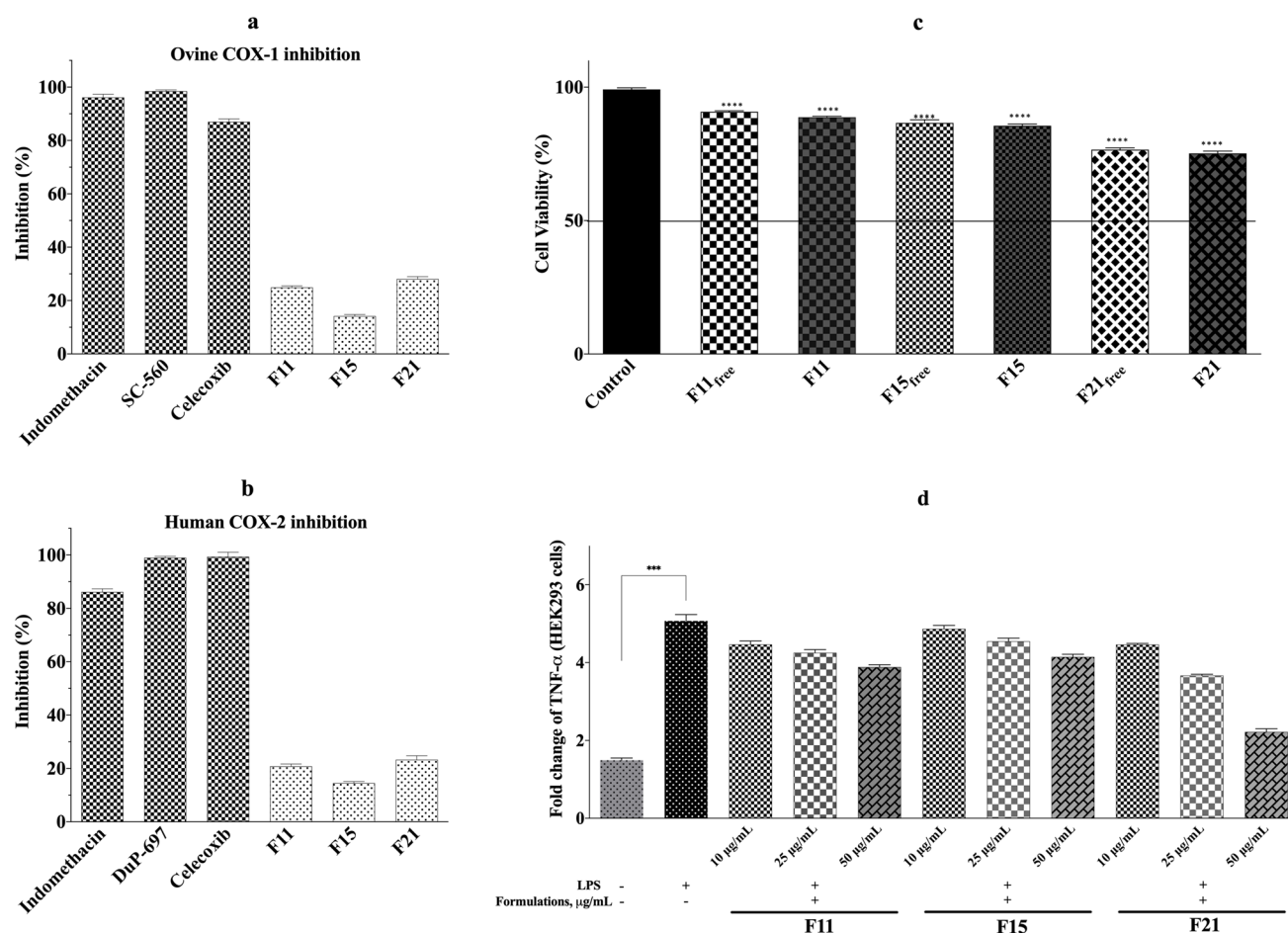


Fig. 6 The graphs represent the results of *in vitro* biological activity and cytotoxicity studies ($n = 3$). **a** COX-1 enzyme inhibition results of positive controls and formulations. SC-560 included in the kit, and two known COX-1 enzyme inhibitors (indomethacin, celecoxib) were used as positive controls. Positive controls and all formulations made a statistically significant difference $p < 0.05$. **b** COX-2 enzyme inhibition results of positive controls and formulations. DuP-697 included in the kit, and two known COX-2 enzyme inhibitors (indomethacin, celecoxib) were used as positive controls. Positive controls and all

formulations made a statistically significant difference $p < 0.05$. **c** Effects of thermosensitive formulations on the viability of HEK293 cells. Cells were treated with 1000 $\mu\text{g}/\text{mL}$ concentration of combinations for 48 h (presenting the mean \pm SD values, **** $p < 0.0001$). **d** Effects of formulations on pro-inflammatory cytokines by LPS-induced HEK293 cells. The data are the means \pm SD ($n = 3$). Statistical analysis was performed by one-way ANOVA with a *t*-test. * indicates a significant difference (at least $p < 0.05$) compared with the LPS-untreated group

Cytotoxicity and *In Vitro* Biologic Activity Studies

The cytotoxicity of BZD-containing formulations was analyzed using different concentrations (1–1000 $\mu\text{g}/\text{mL}$) on HEK293 cells for 48 h by MTT colorimetric assay. As shown in Fig. 6c (1000 $\mu\text{g}/\text{mL}$ concentrations), all tested combinations had cell viability of more than 50%. So, IC_{50} values were not to be found. As a result, while the highest viability was found in the F11 and F11_{free} with a rate of $88.75 \pm 0.67\%$ and $90.79 \pm 0.63\%$, respectively, the lowest viability was in BZD-containing F21 formulation with a rate of $75.21 \pm 1.48\%$. All formulations, both BZD loaded and free, did not have below 70% of viability. While forming the formulations, their contents were determined with

care to non-toxicity. The results of the MTT experiment also confirmed these data.

For the *in vitro* anti-inflammatory study, the COX-1 and COX-2 enzyme inhibitions of the formulations were evaluated. First, all formulations were dissolved in DMSO (less than 1%). Then, inhibition (%) was calculated at different concentrations. When the COX enzyme results were evaluated, below 50% inhibition was not observed even at the highest concentration. IC_{50} values were not calculated for the formulations. The inhibition (%) of the formulations is illustrated in Fig. 6a, b.

To evaluate the effects of the formulation on inflammatory cytokine, the cells were induced with lipopolysaccharide (LPS), and the effects of the formulations were

compared with the induced group. The formulations inhibited the TNF- α ($p < 0.05$) in the LPS-treated HEK293 cells. The expression levels of the parameters viewed as expected in the HEK293 cell were high. The results obtained from the HEK293 cells are illustrated in Fig. 6d. It was seen that TNF- α level increased approximately 5 times in the LPS-induced group compared to the normal control group. The results of the test formulations showed that the TNF- α level decreased ($p \leq 0.001$) when the different non-toxic concentrations (10, 25, 50 $\mu\text{g/mL}$) were compared with the LPS-induced group. For each formulation, TNF- α level was shown to be concentration-dependently inhibited. All formulations showed similar effects with each other. F21 showed the highest effect. Compared with the LPS-induced group, there was a 1.18-, 1.41-, and 2.42-fold inhibition at the 10, 25, and 50 $\mu\text{g/mL}$ concentrations of F21, respectively. Even in the lowest effective F15, a 1.27-fold inhibition was observed at 50 $\mu\text{g/mL}$ concentration. It has been reported that BZD exerts its anti-inflammatory activity by inhibiting the synthesis of pro-inflammatory cytokines such as TNF- α , IL-1, and prostaglandin [2, 76]. Again, Quane stated that BZD acts by inhibiting TNF- α synthesis (EC50 $\mu\text{mol/L}$) in diseases such as inflamed joints [3]. It was seen that the obtained findings were compatible with the literature.

Conclusion

BZD significantly affected the properties of the formulations such as viscosity and gelation temperature. It was observed that the higher viscosity of the formulations had a negative effect on their sprayability. As a result, the viscosity at RT and the gelation temperature of ideal sprayable thermosensitive formulations should be lower than 200 mPa·s and greater than 26°C, respectively. Increasing HPMC and poloxamer amounts had a direct effect on the improvement of bioadhesive ability. While there was no significant difference between the release characteristics of the formulations, it was concluded that increasing HPMC and poloxamer concentrations was effective in BZD accumulation in the skin. Furthermore, while BZD-containing formulations did not show COX activity as expected, its anti-inflammatory activity was demonstrated to be provided by cytokines such as TNF- α . The novel sprayable formulations containing BZD are promising as an easy-to-apply alternative product for topically inflammatory joint disorders, sports injuries, etc.

Acknowledgements The authors would like to thank Humanis (Turkey) for donating benzydamine hydrochloride and BASF Chemicals (Germany) for donating P407, P188, and HPMC K4M.

Author Contribution MDA: supervision, project administration, investigation, methodology, funding acquisition, writing—original draft, and writing—review and editing; EEK: investigation and methodology;

SNB: investigation, methodology, funding acquisition, and writing—original draft

Data Availability The data presented in this study are available on request from the corresponding author.

Declarations

Conflict of Interest The authors declare no competing interests.

References

1. Ardizzoni A, Boaretto G, Pericolini E, Pinetti D, Capezzone de Joannon A, Durando L, et al. Effects of benzydamine and mouth-washes containing benzydamine on *Candida albicans* adhesion, biofilm formation, regrowth, and persistence. *Clin Oral Investig*. 2022;26:3613–25. <https://doi.org/10.1007/s00784-021-04330-85>.
2. Nicolatou-Galitis O, Bossi P, Orlandi E, Bensadoun R-J. The role of benzydamine in prevention and treatment of chemoradiotherapy-induced mucositis. *Support Care Cancer*. 2021;29:5701–9. <https://doi.org/10.1007/s00520-021-06048-5>.
3. Quane PA, Graham GG, Ziegler JB. Pharmacology of benzydamine. *Inflammopharmacology*. 1998;6:95–107. <https://doi.org/10.1007/s10787-998-0026-0>.
4. Arpa MD, Yağcılar AP, Biltekin SN. Novel benzydamine hydrochloride and chlorhexidine gluconate loaded bioadhesive films for local treatment of buccal infections. *J Drug Deliv Sci Technol*. 2023;84. <https://doi.org/10.1016/j.jddst.2023.104497>.
5. Marudova M, Zahariev N, Milenkova S, Pilicheva B, Viraneva A, Yovcheva T. Development and in-vitro characterization of benzydamine loaded chitosan nanoparticles. *Macromol Symp*. 2021;395:1–4. <https://doi.org/10.1002/masy.202000279>.
6. Baldock GA, Brodie RR, Chasseaud LF, Taylor T, Walmsley LM, Catanese B. Pharmacokinetics of benzydamine after intravenous, oral, and topical doses to human subjects. *Biopharm Drug Dispos*. 1991;12:481–92. <https://doi.org/10.1002/bdd.2510120702>.
7. Pilicheva B, Uzunova Y, Bodurov I, Viraneva A, Exner G, Sotirov S, et al. Layer-by-layer self-assembly films for buccal drug delivery: the effect of polymer cross-linking. *J Drug Deliv Sci Technol*. 2020;59. <https://doi.org/10.1016/j.jddst.2020.101897>.
8. Lisciani R, Barcellona PS, Silvestrini B. Researches on the topical activity of benzydamine. *Eur J Pharmacol*. 1968;3:157–62. [https://doi.org/10.1016/0014-2999\(68\)90069-1](https://doi.org/10.1016/0014-2999(68)90069-1).
9. Erol İ, Üstündağ Okur N, Orak D, Sipahi H, Aydın A, Özer Ö. Tazarotene-loaded in situ gels for potential management of psoriasis: biocompatibility, anti-inflammatory and analgesic effect. *Pharm Dev Technol*. 2020;25:909–18. <https://doi.org/10.1080/10837450.2020.1765180>.
10. Gholizadeh H, Messerotti E, Pozzoli M, Cheng S, Traini D, Young P, et al. Application of a thermosensitive in situ gel of chitosan-based nasal spray loaded with tranexamic acid for localised treatment of nasal wounds. *AAPS PharmSciTech*. 2019;20:1–12. <https://doi.org/10.1208/s12249-019-1517-6>.
11. Fan R, Cheng Y, Wang R, Zhang T, Zhang H, Li J, et al. Thermosensitive hydrogels and advances in their application in disease therapy. *Polymers*. 2022;14. <https://doi.org/10.3390/polym14122379>.
12. Aksu NB, Yozgatlı V, Okur ME, Ayla Ş, Yoltaş A, Üstündağ Okur N. Preparation and evaluation of QbD based fusidic acid loaded in situ gel formulations for burn wound treatment. *J Drug Deliv Sci Technol*. 2019;52:110–21. <https://doi.org/10.1016/j.jddst.2019.04.015>.
13. Güven U, Yakut Y, Çakır N, Kayıran S. Thermosensitive in situ gel formulation and characterization studies of *Sambucus ebulus*

- L. extract. *Istanbul J Pharm.* 2023;53:30–8. <https://doi.org/10.26650/IstanbulJPharm.2023.106621>.
14. Wong YL, Pandey M, Choudhury H, Lim WM, Bhattamisra SK, Gorain B. Development of in-situ spray for local delivery of anti-bacterial drug for hidradenitis suppurativa: investigation of alternative formulation. *Polymers.* 2021;13:1–18. <https://doi.org/10.3390/polym13162770>.
 15. Raza H, Shah SU, Ali Z, Khan AU, Rajput IB, Farid A, et al. In vitro and ex vivo evaluation of fluocinolone acetonide–acitretin–coloaded nanostructured lipid carriers for topical treatment of psoriasis. *Gels.* 2022;8:746. <https://doi.org/10.3390/gels8110746>.
 16. Agrawal M, Saraf S, Saraf S, Dubey SK, Puri A, Gupta U, et al. Stimuli-responsive in situ gelling system for nose-to-brain drug delivery. *J Control Release.* 2020;327:235–65. <https://doi.org/10.1016/j.jconrel.2020.07.044>.
 17. Rençber S, Özcan Bülbül E, Üstündağ Okur N, Ay Şenyiğit Z. Preparation and detailed characterization of fusidic acid loaded in situ gel formulations for ophthalmic application. *J Res Pharm.* 2021;25:1–12. <https://doi.org/10.35333/jrp.2021.291>.
 18. Baloglu E, Karavana SY, Senyigit ZA, Guneri T. Rheological and mechanical properties of poloxamer mixtures as a mucoadhesive gel base. *Pharm Dev Technol.* 2011;16:627–36. <https://doi.org/10.3109/10837450.2010.508074>.
 19. Güven UM, Berkman MS, Şenel B, Yazan Y. Development and in vitro/in vivo evaluation of thermo-sensitive in situ gelling systems for ocular allergy. *Brazilian J Pharm Sci.* 2019;55. <https://doi.org/10.1590/s2175-97902019000117511>.
 20. Gratieri T, Gelfuso GM, Rocha EM, Sarmiento VH, de Freitas O, Lopez RFV. A poloxamer/chitosan in situ forming gel with prolonged retention time for ocular delivery. *Eur J Pharm Biopharm.* 2010;75:186–93. <https://doi.org/10.1016/j.ejpb.2010.02.011>.
 21. Barakat NS. In vitro and in vivo characteristics of a thermogelling rectal delivery system of etodolac. *AAPS PharmSciTech.* 2009;10:724–31. <https://doi.org/10.1208/s12249-009-9261-y>.
 22. da Silva JB, Cook MT, Bruschi ML. Thermoresponsive systems composed of poloxamer 407 and HPMC or NaCMC: mechanical, rheological and sol-gel transition analysis. *Carbohydr Polym.* 2020;240:116268. <https://doi.org/10.1016/j.carbpol.2020.116268>.
 23. Kurniawansyah IS, Rusdiana T, Sopyan I, Ramoko H, Wahab HA, Subarnas A. In situ ophthalmic gel forming systems of poloxamer 407 and hydroxypropyl methyl cellulose mixtures for sustained ocular delivery of chloramphenicol: optimization study by factorial design. *Heliyon.* 2020;6(11):e05365. <https://doi.org/10.1016/j.heliyon.2020.e05365>.
 24. Popa L, Ghica MV, Popescu R, Irimia T, Dinu-pîrvu CE. Development and optimization of chitosan-hydroxypropyl methylcellulose in situ gelling systems for ophthalmic delivery of bupivacaine hydrochloride. *Processes.* 2021;9. <https://doi.org/10.3390/pr9101694>.
 25. Pandey P, Cabot PJ, Wallwork B, Panizza BJ, Parekh HS. Formulation, functional evaluation and ex vivo performance of thermoresponsive soluble gels - a platform for therapeutic delivery to mucosal sinus tissue. *Eur J Pharm Sci.* 2017;96:499–507. <https://doi.org/10.1016/j.ejps.2016.10.017>.
 26. Suriyaamporn P, Sahatsapan N, Patrojanasophon P, Opanasopit P, Kumpugdee-Vollrath M, Ngawhirunpat T. Optimization of in situ gel-forming chlorhexidine-encapsulated polymeric nanoparticles using design of experiment for periodontitis. *AAPS PharmSciTech.* 2023;24:161. <https://doi.org/10.1208/s12249-023-02600-0>.
 27. Joshi SC. Sol-gel behavior of hydroxypropyl methylcellulose (HPMC) in ionic media including drug release. *Materials.* 2011;4:1861–905. <https://doi.org/10.3390/ma4101861>.
 28. Bhowmik M, Kumari P, Sarkar G, Bain MK, Bhowmick B, Mollick MMR, et al. Effect of xanthan gum and guar gum on in situ gelling ophthalmic drug delivery system based on poloxamer-407. *Int J Biol Macromol.* 2013;62:117–23. <https://doi.org/10.1016/j.ijbiomac.2013.08.024>.
 29. Üstündağ Okur N, Yozgatlı V, Okur ME, Yoltaş A, Siafaka PI. Improving therapeutic efficacy of voriconazole against fungal keratitis: thermo-sensitive in situ gels as ophthalmic drug carriers. *J Drug Deliv Sci Technol.* 2019;49:323–33. <https://doi.org/10.1016/j.jddst.2018.12.005>.
 30. UstundagOkur N, Yozgatli V, Senyigit Z. Formulation and detailed characterization of voriconazole loaded in situ gels for ocular application. *Ankara Univ Eczac Fak Derg.* 2020;44:33–49. <https://doi.org/10.33483/jfpau.586590>.
 31. Arpa MD, Yoltaş A, Onay Tarlan E, Şenyüz CŞ, Sipahi H, Aydın A, et al. New therapeutic system based on hydrogels for vaginal candidiasis management: formulation–characterization and in vitro evaluation based on vaginal irritation and direct contact test. *Pharm Dev Technol.* 2020;25:1238–48. <https://doi.org/10.1080/10837450.2020.1809457>. (Taylor & Francis).
 32. Dogan A, Başcı NE. Development and validation of RP-HPLC and ultraviolet spectrophotometric methods of analysis for the quantitative determination of chlorhexidine gluconate and benzylamine hydrochloride in pharmaceutical dosage forms. *Curr Pharm Anal.* 2011;7:167–75. <https://doi.org/10.2174/157341211796353228>.
 33. ICH. ICH Harmonised tripartite guideline (2005) validation of analytical procedures: text and methodology Q2(R1). International Conference on Harmonisation of Technical Requirements for Registration of Pharmaceuticals for Human Use, Geneva, 1-13. 2005.
 34. Üstündağ Okur N, Hökenek N, Okur ME, Ayla Ş, Yoltaş A, Siafaka PI, et al. An alternative approach to wound healing field; new composite films from natural polymers for mupirocin dermal delivery. *Saudi Pharm J.* 2019;27:738–52. <https://doi.org/10.1016/j.jsps.2019.04.010>.
 35. Çağlar EŞ, KaraotmarlıGüven G, ÜstündağOkur N. Preparation and characterization of carbopol based hydrogels containing dexpanthenol. *Ankara Univ Eczac Fak Derg.* 2023;47:6–6. <https://doi.org/10.33483/jfpau.1195397>.
 36. Çiftçi H, Arpa MD, Gülaçar İM, Özcan L, Ersoy B. Development and evaluation of mesoporous montmorillonite/magnetite nanocomposites loaded with 5-fluorouracil. *Microporous Mesoporous Mater.* 2020;303. <https://doi.org/10.1016/j.micromeso.2020.110253>.
 37. Ismail A, El-Biyally E, Sakran W. An innovative approach for formulation of rutin tablets targeted for colon cancer treatment. *AAPS PharmSciTech.* 2023;24:1–14. <https://doi.org/10.1208/s12249-023-02518-7>.
 38. Arpa MD, Üstündağ Okur N, Gök MK, Özgümüş S, Cevher E. Chitosan-based buccal mucoadhesive patches to enhance the systemic bioavailability of tizanidine. *Int J Pharm.* 2023;642:123168. <https://doi.org/10.1016/j.ijpharm.2023.123168>.
 39. Arpa MD, Seçen İM, Erim ÜC, Hoş A, ÜstündağOkur N. Azelaic acid loaded chitosan and HPMC based hydrogels for treatment of acne: formulation, characterization, in vitro-ex vivo evaluation. *Pharm Dev Technol.* 2022;27:268–81. <https://doi.org/10.1080/10837450.2022.2038620>.
 40. Üstündağ Okur N, Çağlar EŞ, Arpa MD, Karasulu HY. Preparation and evaluation of novel microemulsion-based hydrogels for dermal delivery of benzocaine. *Pharm Dev Technol.* 2017;22:500–10. <https://doi.org/10.3109/10837450.2015.1131716>.
 41. Sahin Z, Biltekin SN, Yurttas L, Berk B, Özhan Y, Sipahi H, et al. Novel cyanothiouracil and cyanothiocytosine derivatives as concentration-dependent selective inhibitors of U87MG glioblastomas: Adenosine receptor binding and potent PDE4 inhibition. *Eur J Med Chem.* 2021;212. <https://doi.org/10.1016/j.ejmech.2020.113125>.

42. Ertaş M, Biltekin SN, Berk B, Yurttas L, Demirayak Ş. Synthesis of some 5,6-diaryl-1,2,4-triazine derivatives and investigation of their cyclooxygenase (COX) inhibitory activity. *Phosphorus Sulfur Silicon Relat Elem.* 2022;197:1123–35. <https://doi.org/10.1080/10426507.2022.2062756>. (Taylor & Francis).
43. Trivedi MK, Mondal SC, Gangwar M, Jana S. Immunomodulatory potential of nanocurcumin-based formulation. *Inflammopharmacology.* 2017;25:609–19. <https://doi.org/10.1007/s10787-017-0395-3>.
44. Pagano C, Giovagnoli S, Perioli L, Tiralti MC, Ricci M. Development and characterization of mucoadhesive-thermosensitive gels for the treatment of oral mucosa diseases. *Eur J Pharm Sci.* 2020;142. <https://doi.org/10.1016/j.ejps.2019.105125>.
45. Jeong B, Kim SW, Bae YH. Thermosensitive sol-gel reversible hydrogels. *Adv Drug Deliv Rev.* 2012;64:154–62. <https://doi.org/10.1016/j.addr.2012.09.012>.
46. Dahlizar S, Futaki M, Okada A, Kadhum WR, Todo H, Sugibayashi K. Design of a topically applied gel spray formulation with ivermectin using a novel low molecular weight gelling agent, palmitoyl-glycine-histidine, to treat scabies. *Chem Pharm Bull.* 2018;66:327–33. <https://doi.org/10.1248/cpb.c17-00965>.
47. Hsin YK, Thangarajoo T, Choudhury H, Pandey M, Meng LW, Gorain B. Stimuli-responsive in situ spray gel of miconazole nitrate for vaginal candidiasis. *J Pharm Sci.* 2023;112:562–72. <https://doi.org/10.1016/j.xphs.2022.09.002>.
48. Kolawole OM, Cook MT. In situ gelling drug delivery systems for topical drug delivery. *Eur J Pharm Biopharm.* 2023;184:36–49. <https://doi.org/10.1016/j.ejpb.2023.01.007>.
49. Rincón M, Silva-Abreu M, Espinoza LC, Sosa L, Calpena AC, Rodríguez-Lagunas MJ, et al. Enhanced transdermal delivery of pranoprofen using a thermo-reversible hydrogel loaded with lipid nanocarriers for the treatment of local inflammation. *Pharmaceuticals.* 2022;15. <https://doi.org/10.3390/ph15010022>.
50. Ban E, Park M, Jeong S, Kwon T, Kim EH, Jung K, et al. Poloxamer-based thermoreversible gel for topical delivery of emodin: influence of P407 and P188 on solubility of emodin and its application in cellular activity screening. *Molecules.* 2017;22. <https://doi.org/10.3390/molecules22020246>.
51. Mura P, Mennini N, Nativi C, Richichi B. In situ mucoadhesive-thermosensitive liposomal gel as a novel vehicle for nasal extended delivery of opiorphin. *Eur J Pharm Biopharm.* 2018;122:54–61. <https://doi.org/10.1016/j.ejpb.2017.10.008>.
52. Fathalla Z, Mustafa WW, Abdelkader H, Moharram H, Sabry AM, Alany RG. Hybrid thermosensitive-mucoadhesive in situ forming gels for enhanced corneal wound healing effect of L-carnosine. *Drug Deliv.* 2022;29:374–85. <https://doi.org/10.1080/10717544.2021.2023236>.
53. Ali SM, Yosipovitch G. Skin pH: from basic science to basic skin care. *Acta Derm Venereol.* 2013;93:261–7. <https://doi.org/10.2340/00015555-1531>.
54. Gözcü S, Polat KH. Thermosensitive *in situ* gelling system for dermal drug delivery of rutin. *Turkish J Pharm Sci.* 2022;20:78–83. <https://doi.org/10.4274/tjps.galenos.2022.00334>.
55. Tuğcu-Demiröz F. Development of in situ poloxamer-chitosan hydrogels for vaginal drug delivery of benzydamine hydrochloride: textural, mucoadhesive and in vitro release properties. *Marmara Pharm J.* 2017;21:762–70. <https://doi.org/10.12991/mpj.2017.3>.
56. Chen IC, Su CY, Chen PY, Hoang TC, Tsou YS, Fang HW. Investigation and characterization of factors affecting rheological properties of poloxamer-based thermo-sensitive hydrogel. *Polymers.* 2022;14. <https://doi.org/10.3390/polym14245353>.
57. Hirun N, Kraisit P, Tantishaiyakul V. Thermosensitive polymer blend composed of poloxamer 407, poloxamer 188 and polycarbophil for the use as mucoadhesive in situ gel. *polymers.* 2022;14. <https://doi.org/10.3390/polym14091836>.
58. Akkari ACS, Papini JZB, Garcia GK, Franco MKKD, Cavalcanti LP, Gasperini A, et al. Poloxamer 407/188 binary thermosensitive hydrogels as delivery systems for infiltrative local anesthesia: physico-chemical characterization and pharmacological evaluation. *Mater Sci Eng C.* 2016;68:299–307. <https://doi.org/10.1016/j.msec.2016.05.088>.
59. Soliman GM, Fetih G, Abbas AM. Thermosensitive bioadhesive gels for the vaginal delivery of sildenafil citrate: in vitro characterization and clinical evaluation in women using clomiphene citrate for induction of ovulation. *Drug Dev Ind Pharm.* 2017;43:399–408. <https://doi.org/10.1080/03639045.2016.1254239>.
60. Parhi R. Development and optimization of Pluronic® F127 and HPMC based thermosensitive gel for the skin delivery of metoprolol succinate. *J Drug Deliv Sci Technol.* 2016;36:23–33. <https://doi.org/10.1016/j.jddst.2016.09.004>.
61. Choi H-G, Jung J-H, Ryu J-M, Yoon S-J, Oh Y-K, Kim C-K. Development of in situ-gelling and mucoadhesive acetaminophen liquid suppository. *Int J Pharm.* 1998;165:33–44. [https://doi.org/10.1016/S0378-5173\(97\)00386-4](https://doi.org/10.1016/S0378-5173(97)00386-4).
62. Khan S, Minhas MU, Tekko IA, Donnelly RF, Thakur RRS. Evaluation of microneedles-assisted in situ depot forming poloxamer gels for sustained transdermal drug delivery. *Drug Deliv Transl Res.* 2019;9:764–82. <https://doi.org/10.1007/s13346-019-00617-2>.
63. Annaji M, Mita N, Rangari S, Aldawsari MF, Alsaqr A, Poudel I, et al. Enhanced topical Co-delivery of acyclovir and lidocaine gel formulation across dermatomed human skin. *AAPS PharmSciTech.* 2022;23. <https://doi.org/10.1208/s12249-022-02458-8>.
64. Bhuyan MM, Okabe H, Hidaka Y, Dafader NC, Rahman N, Hara K. Synthesis of pectin-N, N-dimethyl acrylamide hydrogel by gamma radiation and application in drug delivery (in vitro). *J Macromol Sci Part A Pure Appl Chem.* 2018;55:369–76. <https://doi.org/10.1080/10601325.2018.1442177>.
65. Al homsi R, Eltahir S, Jagal J, Ali Abdelkareem M, Ghoneim MM, Rawas-Qalaji MM, et al. Thermosensitive injectable graphene oxide/chitosan-based nanocomposite hydrogels for controlling the in vivo release of bupivacaine hydrochloride. *Int J Pharm.* 2022;621:121786. <https://doi.org/10.1016/j.ijpharm.2022.121786>.
66. Sathyanarayana SD, Rompicherla NC, Vadakkepushpakath AN, Nayak P. Development of thermosensitive ophthalmic in situ gels of bimatoprost for glaucoma therapy. *Indian J Pharm Educ Res.* 2020;54:S154-62. <https://doi.org/10.5530/ijper.54.2s.71>.
67. Pham DT, Phewchan P, Navesit K, Chokamonsirikun A, Khemwong T, Tiyaboonthai W. Development of metronidazole-loaded in situ thermosensitive hydrogel for periodontitis treatment. *Turk J Pharm Sci.* 2021;18:510–6. <https://doi.org/10.4274/tjps.galenos.2020.09623>.
68. Guerra-Ponce WL, Gracia-Vásquez SL, González-Barranco P, Camacho-Mora IA, Gracia-Vásquez YA, Orozco-Beltrán E, et al. In vitro evaluation of sustained released matrix tablets containing ibuprofen: a model poorly water-soluble drug. *Braz J Pharm Sci.* 2016;52:751–60. <https://doi.org/10.1590/S1984-8250201600400020>.
69. Kapileshwari GR, Barve AR, Kumar L, Bhide PJ, Joshi M, Shirodkar RK. Novel drug delivery system of luliconazole - formulation and characterisation. *J Drug Deliv Sci Technol.* 2020;55:101302. <https://doi.org/10.1016/j.jddst.2019.101302>.
70. Arafa MG, Ayoub BM. DOE optimization of nano-based carrier of pregabalin as hydrogel: new therapeutic & chemometric approaches for controlled drug delivery systems. *Sci Rep.* 2017;7:1–15. <https://doi.org/10.1038/srep41503>.
71. Feyissa Z, Edossa GD, Bedasa TB, Inki LG. Fabrication of pH-responsive chitosan/polyvinylpyrrolidone hydrogels for controlled release of metronidazole and antibacterial properties. *Int J Polym Sci.* 2023;1205092. <https://doi.org/10.1155/2023/1205092>.

72. Barakat NS. Optimization of physical characterization, skin permeation of naproxen from glycofurol-based topical gel. *Asian J Pharm.* 2010;4:154–62. <https://doi.org/10.22377/ajp.v4i2.140>.
73. Alkilani AZ, McCrudden MTC, Donnelly RF. Transdermal drug delivery: innovative pharmaceutical developments based on disruption of the barrier properties of the stratum corneum. *Pharmaceutics.* 2015;7:438–70. <https://doi.org/10.3390/pharmaceutics7040438>.
74. Latif MS, Azad AK, Nawaz A, Rashid SA, Rahman MH, Al Omar SY, et al. Ethyl cellulose and hydroxypropyl methyl cellulose blended methotrexate-loaded transdermal patches: In vitro and ex vivo. *Polymers.* 2021;13. <https://doi.org/10.3390/polym13203455>.
75. Binder L, Mazál J, Petz R, Klang V, Valenta C. The role of viscosity on skin penetration from cellulose ether-based hydrogels. *Ski Res Technol.* 2019;25:725–34. <https://doi.org/10.1111/srt.12709>.
76. Mehravaran M, Haeri A, Rabbani S, Mortazavi SA, Torshabi M. Preparation and characterization of benzydamine hydrochloride-loaded lyophilized mucoadhesive wafers for the treatment of oral mucositis. *J Drug Deliv Sci Technol.* 2022;78. <https://doi.org/10.1016/j.jddst.2022.103944>.

Publisher's Note Springer Nature remains neutral with regard to jurisdictional claims in published maps and institutional affiliations.

Springer Nature or its licensor (e.g. a society or other partner) holds exclusive rights to this article under a publishing agreement with the author(s) or other rightsholder(s); author self-archiving of the accepted manuscript version of this article is solely governed by the terms of such publishing agreement and applicable law.